

# REPRODUCTION OF SLOPE FAILURE DUE TO RAINFALL IN A CENTRIFUGE MODEL TEST

Ryotaro Tomooka  
Graduate School of  
Integrative Science and  
Engineering Civil  
Engineering  
Tokyo City University  
Tokyo, Japan  
g1981629@tcu.ac.jp

Kazuya Itoh  
Dept. of Urban and  
Civil Engineering  
Tokyo City University  
Tokyo, Japan  
itok@tcu.ac.jp

Tsuyoshi Tanaka  
Dept. of Urban and  
Civil Engineering  
Tokyo City University  
Tokyo, Japan  
ttanaka@tcu.ac.jp

Naoaki Suemasa  
Dept. of Urban and  
Civil Engineering  
Tokyo City University  
Tokyo, Japan  
nsuemasa@tcu.ac.jp

**Abstract**— Recently, a lot of terrible damage, such as a slope failure, has been caused by earthquakes or torrential rains. In this paper, a centrifugal model was used to reproduce a slope failure during rainfall. In the centrifugal experiment, the rainfall trajectory changed due to the effect of Coriolis force. However, when the conditions, specifically height and angle of the raindrop were adjusted, it was possible to make the rainfall uniform and cause a slope failure without gully erosion.

**Keywords**—*Slope failure, Rainfall, Coriolis force, Centrifugal modelling*

## I. INTRODUCTION

In recent years, many disasters have occurred due to slope failures. There are artificial and natural phenomena as factors that destabilize slopes. Natural phenomena include soil weathering and weight increase due to rainfall and earthquakes. In order to clarify the mechanism of a slope failure caused by rainfall, this study focuses on development of a centrifugal rainfall generation system and slope failure experiment during rainfall using the system. This report describes (1) the rainfall trajectory calculated by the Coriolis force, (2) the rainfall distribution in 1G and centrifugal acceleration field using the developed centrifugal rainfall generation system, and (3) slope failure situation during rainfall under 50 G acceleration.

## II. CALCULATION OF RAINDROP TRAJECTORY BY CORIOLIS FORCE

### A. Literature review of centrifuge rainfall modelling

When performing a centrifugal rainfall model experiment, the rainfall trajectory is curved under the effect of the Coriolis force. The Coriolis force is a virtual force caused by the deviation between the rotating coordinate system and the stationary coordinate system at the time when a force acts on the moving object in the direction opposite to the rotating direction in the centrifugal field. Tamate et al. [1] succeeded in achieving uniform rainfall by finely

adjusting the angle of the water spray nozzle by substituting the effective radius of the centrifugal device, the rotation speed, the rotation radius of the spray location, the initial rainfall rate etc. from the equation of motion of the rotating coordinate system. In addition, Caicedo et al. [2] analyzed raindrop trajectories in the centrifugal field and compared the results with experimental results. The change of raindrop fall trajectory by Coriolis force depends on the rotation speed. The effective radius of the centrifugal model experiment equipment was 2.3 m for Tamate et al. [1][2] and 1.4 m for Caicedo et al. [3]. On the other hand, the effective radius of the cup type swing-up centrifugal loading device owned by Tokyo City University (TCU Mark-II centrifuge) is 0.35 m, and in order to make the centrifugal acceleration 50 G, it is necessary to make the rotational speed larger than that of the large device. Therefore, the rainfall trajectory changes were calculated in the 50G centrifugal acceleration field using this device. The calculation was made based on the free fall simulation in the centrifugal field performed by Itoh et al. [4]. As the force of gravity is added to the centrifugal acceleration in the centrifugal model experiment, the swing-up angle is not 90 degrees. Based on it, a three-dimensional study was conducted by Itoh et al. [4] thereafter.

### B. Kinematics of free fall in a rotation frame

While a centrifuge is an extremely convenient method of generating an artificial high-gravitational acceleration field, problems are associated with its rotation about a fixed axis. One of these problems is the Coriolis acceleration, which develops when there is radial movement in the model under hyper gravity, in the plane of rotation. In general, if a structure (particle, section of failing slope) has a significant velocity relative to the centrifuge platform, the dynamics must include Coriolis effects. The effect of Coriolis forces on centrifuge model tests has been

pointed out in many papers (e.g., Schofield [5], Tan and Scott [6] and Steedman and Zeng [7]).

This section presents a comparison between the experimental and theoretical movements of the free falling to examine the Coriolis effects. The theoretical movement of free falling, when the projectile is assumed still to be in rotational acceleration field, is solved, as shown below.

Consider a raindrop of mass  $m$  and position relative to  $O$ , as shown in Figs. 1. In the inertial frame 'S', the raindrop obeys Newton's second law of motion,

$$m \left( \frac{d^2 \mathbf{r}}{dt^2} \right)_S = \mathbf{F} \quad (1)$$

where  $\mathbf{F}$  denotes the net force on the raindrop, the vector sum of all forces identified in the inertial frame. The derivative on the left is the derivative evaluated by observers in the inertial frame 'S'.

$$\left( \frac{d\mathbf{r}}{dt} \right)_S = \left( \frac{d\mathbf{r}}{dt} \right)_R + \boldsymbol{\Omega} \times \mathbf{r} \quad (2)$$

from the velocity transformation equation (2) it follows that,

$$\left( \frac{d^2 \mathbf{r}}{dt^2} \right)_S = \left( \frac{d^2 \mathbf{r}}{dt^2} \right)_R + 2\boldsymbol{\Omega} \times \left( \frac{d\mathbf{r}}{dt} \right)_R + \boldsymbol{\Omega} \times (\boldsymbol{\Omega} \times \mathbf{r}) \quad (3)$$

It follows from the acceleration transformation in equation (3), that, when the same motion is observed from the rotation frame 'R', equation (1) is replaced by the transformed equation of motion, as follows;

$$m \frac{d^2 \mathbf{r}}{dt^2} = \mathbf{F} - 2m\boldsymbol{\Omega} \times \frac{d\mathbf{r}}{dt} - m\boldsymbol{\Omega} \times (\boldsymbol{\Omega} \times \mathbf{r}) \quad (4)$$

where,  $\mathbf{F}$  denotes the sum of all the forces as identified in any inertial frame. The equation of motion in a rotation frame is similar to Newton's second law, except that in this case there are two extra terms on the force side of the equation. The first of these extra terms is called the "Coriolis force", and the second is the so-called "centrifugal force".

After dividing equation (4) by  $m$ , the equation of motion becomes;

$$\frac{d^2 \mathbf{r}}{dt^2} = \frac{\mathbf{F}}{m} - 2\boldsymbol{\Omega} \times \frac{d\mathbf{r}}{dt} - \boldsymbol{\Omega} \times (\boldsymbol{\Omega} \times \mathbf{r}) \quad (5)$$

The origin on the release point at the position  $\mathbf{r}$ , as shown in Fig. 1 is chosen in this study. According to these axes ((X, Y, Z) and (x, y, z)), the equation of motion is resolved into its three components. The components of  $\mathbf{R}$ ,  $\boldsymbol{\Omega}$ , and  $\mathbf{F}$  are

$$\mathbf{R} = (x, y, z + r)$$

$$\boldsymbol{\Omega} = (0, -\Omega \sin \phi, \Omega \cos \phi)$$

$$\mathbf{F} = (F_x, F_y, F_z) = (0, -mg \sin \phi, mg \cos \phi)$$

The equation of motion (5) resolves into the following three equations:  $\frac{d^2 x}{dt^2} = \frac{F_x}{m} - 2\Omega \left( \frac{dz}{dt} \sin \phi + \frac{dy}{dt} \cos \phi \right) + \Omega^2 x$

$$\frac{d^2 y}{dt^2} = \frac{F_y}{m} - 2\Omega \frac{dx}{dt} \cos \phi + \Omega^2 ((z + r) \sin \phi - y \cos \phi) \cos \phi$$

$$\frac{d^2 z}{dt^2} = \frac{F_z}{m} - 2\Omega \frac{dx}{dt} \sin \phi + \Omega^2 ((z + r) \sin \phi - y \cos \phi) \sin \phi$$

(6)

To obtain the solution of these ordinary differential equations, a fourth order Runge-Kutta method was used in this study. With the initial condition (at  $t=0$ ):

$$x = y = z = 0$$

$$\frac{dx}{dt} = v_{\text{spray}-x}, \frac{dy}{dt} = v_{\text{spray}-y}, \frac{dz}{dt} = v_{\text{spray}-z}$$

Fig. 2 shows a schematic view (plan view) of the installation location of the model container in the centrifuge and the direction of rotation. An acrylic window is installed on the front of the container for observing the model during the centrifuge test. Coriolis force causes the fall path of rainfall to bend toward the acrylic side. A liquid pressure type spray nozzle (spray angle: 80 degrees) is used as a mechanism of the centrifugal rainfall generation system. The Fig. 3 shows the raindrop falling trajectory at initial velocity of 15 m / s and with a height of up to 80 mm. Since the angle sprayed from the nozzle is 80 degrees, the red plot is set to -40 degrees, and the blue plot is set to 40 degrees. As seen from the figure, both the red and blue plots are bent in the positive direction, indicating the rainfall is asymmetrical.

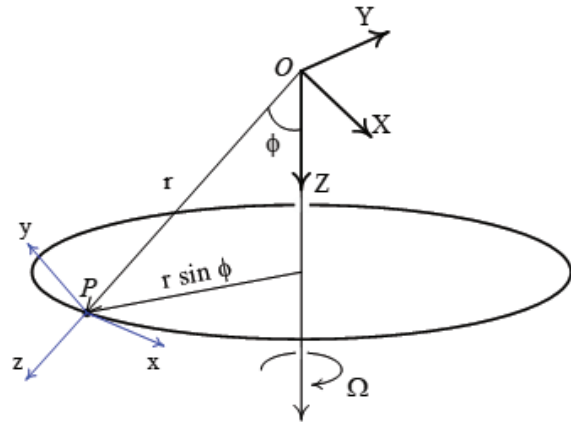


Fig.1. Coordinate system for studying motion from rotation frame

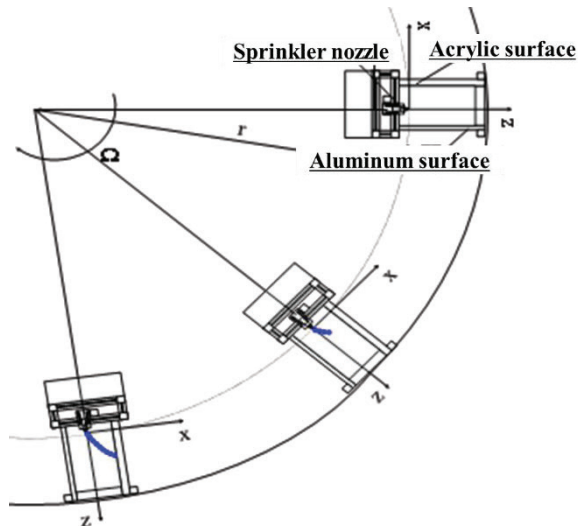


Fig.2. Conceptual drawing of model container installation location and rotation direction (plan view)

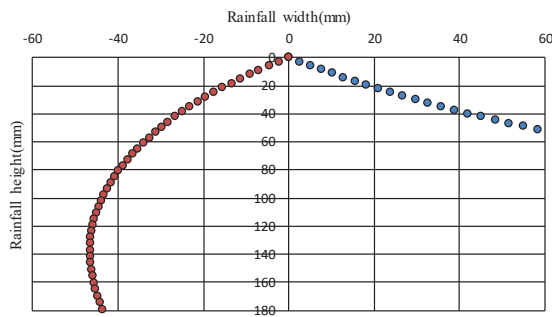


Fig.3. Raindrop fall trail

### III. RAINFALL DISTRIBUTION MEASUREMENT BY CENTRIFUGAL FIELD RAINFALL SYSTEM

#### A. Centrifugal rainfall generation system

The condition of rainfall distribution was confirmed using the centrifugal rainfall generation system. The spray nozzle used (Ikeuchi product: fine mist generation ultra-compact nozzle, Flat Spray SCBIMV series nozzles) is a two-fluid nozzle that generates fine mist with an average particle diameter of 100  $\mu\text{m}$  or less, and the spray shape has a spray angle of 80 degrees. It is a liquid pressure type that sprays a spray liquid under a pressure of about 0.1 to 0.3 MPa and has a wide flow control range. In this experiment, 0.3 MPa is given.

#### B. Experiment set-up

An aluminum model container with inner sizes of 300 mm in width, 120 mm in breadth, and 200 mm in height was used in this study. Fig. 4 shows schematic view of the centrifuge model test setup in this study. Small beakers ( $\phi=16\text{mm}\times 16\text{mm}$ ) were installed at 30 mm from the bottom of the model container to check the rainfall distribution. The experimental setup is shown below. Styrofoam was placed at the bottom of the model container, and beakers were placed in 4 vertical rows and 11 in lateral rows and each distance between

the centers of the beakers was 30 mm. Two spray nozzles were

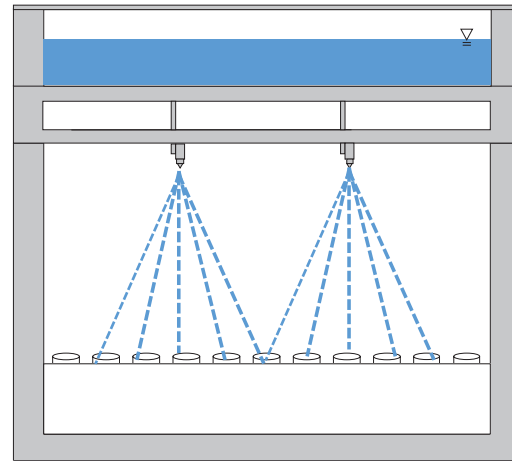


Fig.4. Schematic view of the centrifuge model test setup

placed at the center of the model container (depth 60 mm), and the distance from the spray nozzle to the beaker was 180 mm. Water was sprayed for 10 minutes by applying predetermined air pressure both in the gravity field (1G, Non Coriolis force condition) and in the 50G centrifugal acceleration field. After that, the amount of water accumulated in each small beaker was measured and converted into hourly amount to confirm the rainfall distribution situation. Table 1 shows the experimental cases conducted this time.

Table.1. Experiment case

case	Height to the nozzle	Experimental situation
1	180mm	Gravity field (1G)
2	180mm	Centrifugal acceleration 50G field
3	150mm	Centrifugal acceleration 50G field

Case 1 and Case 2 were set to compare the difference between the gravity field (1G) and 50 G field, and the drop position in Case 3 was lowered by 30 mm to confirm the difference depends on the drop height.

#### C. Experimental result

Figure. 5, 6 and 7 show the distributions of rainfall in Case 1, Case 2 and Case 3, respectively. In the figures, the + marks represent the nozzles and the white circles represent the beakers. As known from the two figures 4 and 5, it can be seen that the rainfall in the 50G field is ranged more in the acrylic side than aluminum side compared with that in the gravity field. This is because the raindrop fall trajectory is curved to the acrylic side by the effect of Coriolis force. In Case 3, the height of the nozzle was 150 mm lowered by 30 mm than other cases in order to reduce the influence of Coriolis force. Compared with Fig. 5, the rainfall distribution is concentrated in the parts near the right under the nozzles in Fig. 6. This indicates that water was accumulated in the beakers under the nozzles before the rainfall trajectory was bent due to the effect of Coriolis force. It was confirmed that the curvature of the

raindrop fall trajectory due to the Coriolis force can be suppressed to some extent by lowering the nozzle height. Based on the above results, the drop height was lowered to 80 mm in the following slope failure experiment.

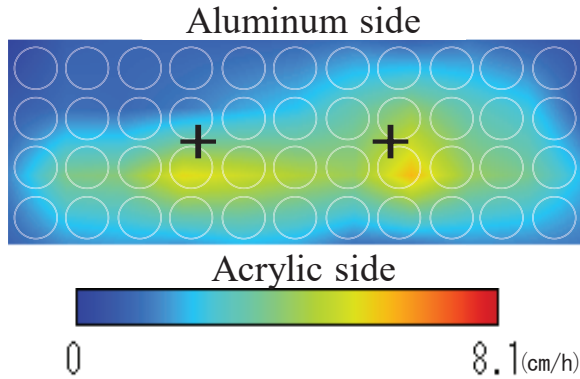


Fig. 5. Rainfall distribution (case 1)

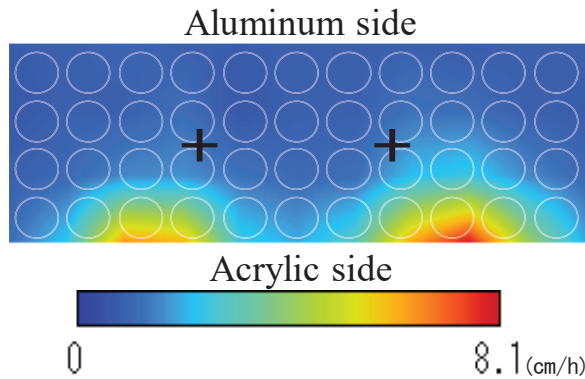


Fig. 6. Rainfall distribution (case 2)

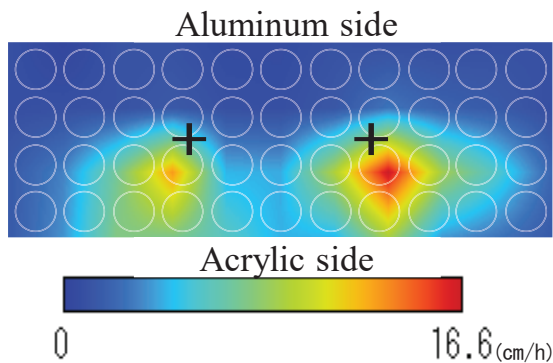


Fig. 7. Rainfall distribution (case 3)

#### IV. CENTRIFUGE MODEL TEST OF SLOPE FAILURE DUE TO RAINFALL

##### A. Outline of experiment

The sample used for the model slope was Ao clay and silica sand No. 7 with a weight ratio of 3 : 1, water content  $w = 13\%$  and wet density  $\rho_t = 1.5\text{g/cm}^3$ , which was divided into two layers and compacted statically using Belofram cylinder. The range of particle size of the mixture soil is sand: 30.97%, silt: 34.69%, and clay: 34.34%. The model ground was prepared, cutting out a slope shape with an angle of 60 degrees and height of 90 mm using a plywood form. Two spray nozzles were

located right above the slope and the top of slope. In order to prevent water droplets flowing down from the side walls into the ground, rain gutters were installed on the side walls to drain the water. At the acceleration of 50G, the spraying started and continued until slope failure occurred and became motionless. As for measurement, settlement of top of slope was detected by displacement transducer and a video camera for confirming the state of collapse of the slope. Figure. 8 shows the installation conditions of the model container and various measuring instruments used.

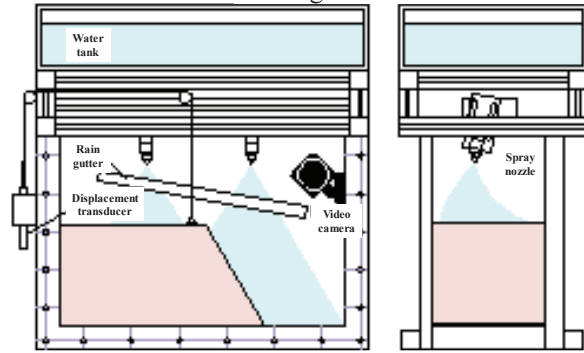


Fig.8. Experimental setup

Since there was no place to install the displacement transducer in the model container, it was installed on the outside, attached with a fishline which was connected to the displacement meter outside and to two pulleys outside and inside to measure the settlement. A heavier weight than the rod was attached to the tip of fishline so as not to sag. The video camera (Go Pro HERO 5 Session) was installed on the opposite side to the slope face so that deformation of the slope could be easily observed. Table 2 shows the results of the experiment and the deformation of the ground surface after the experiment. Cases 1 and 2 are cases where the drop heights from the spray nozzle to the ground were different and Case 3 was the case where the direction of the spray nozzle face was inclined to the aluminum side about 20 degrees. The displacement transducer was installed in Cases 2 and 3, however, a defect occurred during the measurement in Case 3.

##### B. Experiment result

Table 2 shows photographs of slope deformation on the ground surface after the experiment. In Case 1, the slope is deformed on the acrylic side while no large deformation is seen on the aluminum side. It can be seen that the ground surface has cracks in the perpendicular direction to the slope. This is because the ground surface was not evenly rained by the fact that the rainfall range was bent by Coriolis force and concentrated only on the acrylic side. Therefore, in Case 2, the height of the spray nozzle was lowered by 30 mm and the drop height was 50 mm. Compared with Case 1, it is clear that cracks in the perpendicular direction to the slope moved to the aluminum side slightly from the center in Case 2. It is considered that the rainfall range moved from the acrylic side to the central part by lowering the position of the spray nozzle. Fig. 9 shows time history of settlement of the top of slope (Fig. 9 (a)), and deformation at 0 seconds (Fig. 9



(c)), 500 seconds (Fig. 9 (d)), 1500 seconds (Fig. 9 (e)), and 2500 seconds (Fig. 9 (f) and (b)) after rainfall started in Case 2. Here, the rainfall start time is defined as 0 second. As seen from the graph, settlement of top of slope started at approximately 500 seconds and the amount of subsidence increased significantly between 500 and 1500 seconds.

Slope failure started from 500 seconds and collapsed area expanded until 1500 seconds. After 1500 seconds, the ground surface sank gradually without major collapse.

In Case 2 and Case 3, the water contents near the ground surface were measured after the experiment. Fig.10 shows the measurement positions of water content and Table 4 shows the measurement results of water content. The water content at the points 1 and 4 in Case 2 were compared, where cracks occurred in the middle between. According to the Table 4, water content ratios at the points 1 and 4 after experiment are higher than those of the initial condition, however, the point 4 on the aluminum side is higher than the point 1. From the results of the shape of slope failure and the water content, it was suggested that changing the height of the spray nozzle did not evenly give the rainfall range. However, lowering the height of the nozzle more may cause gully erosion. In Case 3, therefore, the direction of the spray nozzle face was inclined to the aluminum side with the same spray nozzle position as Case 2. Compared to the other cases, the center of the model container was deformed the most and cracks were formed on both aluminum and acrylic sides in Case 3. When the water content on the ground surface were measured after the experiment was completed, the water content at the points 1 to 4 near the top of slope were almost the same. From this, it was possible to correct the deviation of the rainfall range due to the influence of the Coriolis force. However, as the water content ratios at the points 5 and 6 on the far side of the slope were lower than those at the points 1 to 4, it was found the rainfall range was different depend on the

areas. From this, there is a possibility that increasing the number of nozzles could lead more uniform rainfall range. However, as a whole, since a slope failure and collapse successfully occurred with no gully erosion, sufficiently fine and uniform rainfall was made on the area from the points 1 to 4 and over the slope when providing a proper raindrop height in this experiment.

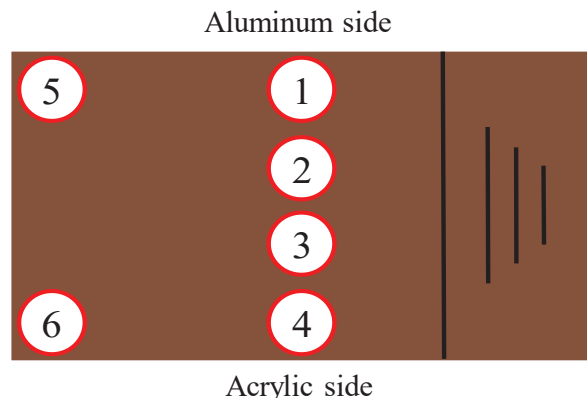


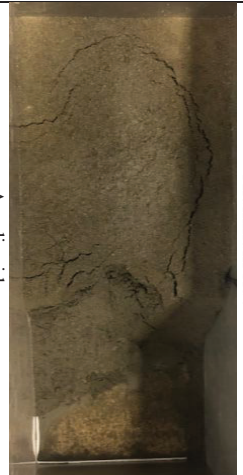


Fig.10. Measurement positions of water content

Table 4. Water content

Case	Measurement position of water content (%)					
	1	2	34	4	5	6
2	19.9	Non	Non	26.2	Non	Non
3	24.2	24.7	25.8	25.1	19.2	20.3

Table 2. Experimental case

case	1	2	3
Drop height	80mm	50mm	50mm
Nozzle orientation	directly below	directly below	Acrylic side
Displacement gauge		○	×
Ground surface condition after the experiment (Lower side is slope)			
			

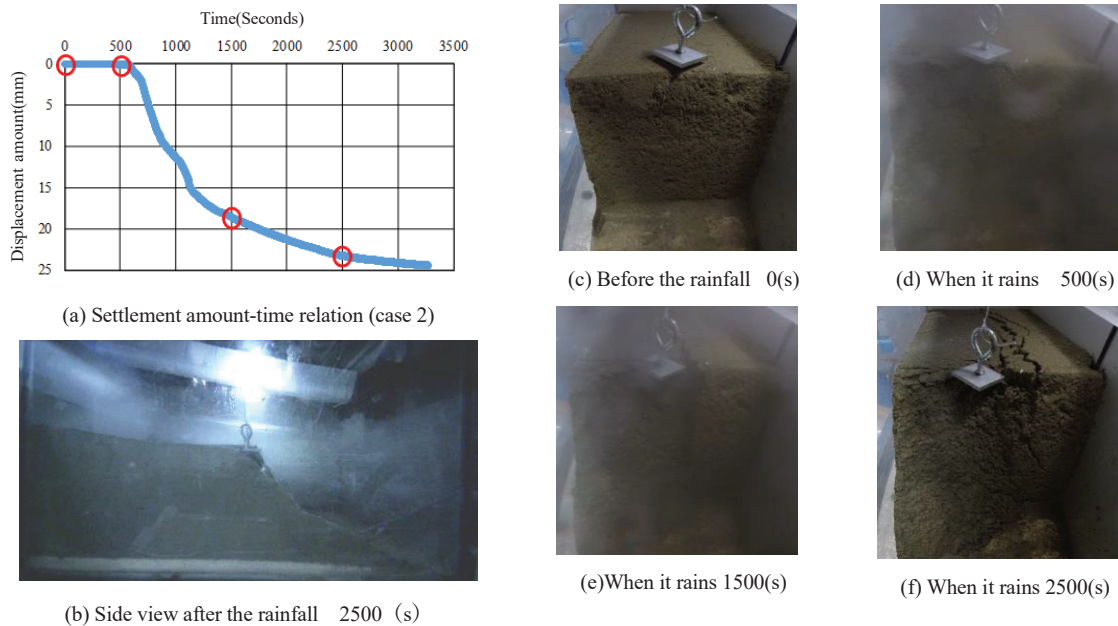


Fig.9. Settlement amount-time relation and deformation situation

## V. CONCLUSIONS

In this paper, the raindrop trajectory by the effect of Coriolis force was calculated and the rainfall distribution in the centrifugal field using rainfall generation system and the centrifugal model test of slope failure during rainfall were described. In the centrifugal field (rotational field), it was found that it was necessary to lower the raindrop height and to change the angle of the spray nozzle face because the rainfall trajectory was bent by the Coriolis force acting. Although slope failure occurred in the centrifugal rainfall experiment, the difference in slope deformation and in the water content were confirmed. In order to correct the deviation of the rainfall trajectory by the effect of Coriolis force and reproduce more uniform rainfall, further improvement is needed such as increasing the number of nozzles or changing the positions in the future.

## REFERENCES

- [1] S. Tamate, N. Itoh, and A. Endo "Experimental Analysis on Shallow Failure of Slope in Consideration of Relationship between Ground Permeability and Precipitation Intensity," *Specific Research Reports of the National Institute of Occupational Safety and Health*, JNIOHS-SRR-NO35, 2007 (in Japanese).
- [2] S. Tamate, N. Suemasa, and T. Katada, "Simulation of precipitation on centrifuge models of slopes," *International Journal of Physical Modelling in Geotechnics*, Vol. 12, No. 3, pp.89-101, 2012.
- [3] B. Caicedo, L. Thorel, and J. Tristanocho, "Mathematical and physical modelling of rainfall in centrifuge," *International Journal of Physical Modelling in Geotechnics*, Vol. 15, No. 3, pp. 150~164, 2015.
- [4] K. Itoh, Y. Toyosawa, and O. Kusakabe, "Centrifugal modelling of rockfall events," *International Journal of Physical Modelling in Geotechnics*, Vol. 9, pp. 1~22, 2009.

- [5] A. N. Schofield "Cambridge Geotechnical Centrifuge Operations," *Géotechnique*, Vol. 30, No. 3, pp. 227-268, 1980.
- [6] T. S. Tan, and R. F. Scott "Centrifuge scaling considerations for fluid-particle systems," *Géotechnique*, Vol. 35, No. 4, pp. 461-470, 1985.
- [7] R. S. Steedman, and X. Zeng, Chapter "Dynamics," *Geotechnical Centrifuge Technology* (ed. R. N. Taylor), Blackie Academic & Professional, London. 1995